The University of Adelaide

Department of Mechanical Engineering

Control and Optimisation of Mixing and Combustion from a Precessing Jet Nozzle

Ph.D. Thesis

Jordan James Parham

December 2000

Abstract

The present study seeks to examine the effects of co-flow, confinement and a shaping jet on the mixing and combustion characteristics of a precessing jet flow. In particular, scientific analysis is used to investigate the physical mechanisms by which the control and optimisation of heat transfer and pollutant emissions from natural gas burners for rotary kilns can be achieved. To achieve these aims, a range of experimental techniques in reacting, non-reacting, confined and unconfined conditions have been employed. The precessing jet, in conjunction with a shaping jet, is shown to provide continuous control of mixing characteristics and corresponding combustion characteristics. Hence the optimum mixing characteristics for the maximum heat transfer and minimum emissions and the conditions under which the precessing jet nozzle produces such mixing characteristics are determined. A scaling procedure is also proposed for the precessing jet nozzle that, for the first time, provides a method to relate the results of small-scale isothermal mixing experiments to operating rotary kilns.

Flow visualisation using a two colour planar laser-induced fluorescence technique in an unconfined, isothermal environment is used to demonstrate that a central axial jet is the most effective form of shaping jet for controlling the mixing from a precessing jet nozzle. The characteristics of the combined jet flow are shown, by a semi-quantitative image processing technique, to be controlled by the ratio of the central axial jet momentum to the combined jet momentum, denoted by $\Gamma_{CAJ}=G_{CAJ}/(G_{PJ}+G_{CAJ})$. The flow visualisation results also demonstrate that, when the momentum ratio is in the range $0\leq \Gamma_{CAJ} \leq 0.2$, corresponding to low proportions of flow through the central axial jet, the combined flow field visually appears to be "precessing jet dominated". For momentum ratios in the range $0.23\leq \Gamma_{CAJ} \leq 1$, the flow appears visually to be dominated by the features of the central axial jet.

The effect of a central axial jet on the characteristics of a precessing jet flame is assessed in an unconfined environment by recording the visible flame luminescence photographically. The results demonstrate that a significant change in the flame volume, length and width is achieved by varying the proportion of central axial jet to total flow rate and hence the momentum ratio, Γ_{CAJ}. These parameters were correlated with changes in the global residence time, radiant fraction and NO_x emissions based on scaling criteria from the literature. These correlations suggest that, consistent with the flow visualisation results, the momentum ratio, Γ_{CAJ}, controls the combustion characteristics, which in turn change significantly in the precessing jet and central axial jet dominated flow regimes.

Confined combustion experiments are undertaken in a pilot-scale cement kiln simulator to quantify the heat flux and NO_x emission characteristics as a function of the combined precessing jet and central axial jet flows and to compare them with that of a conventional burner in a well controlled, confined facility. These experiments demonstrate that the central axial jet provides good control over the heat flux profile, consistent with the experience in industrial installations. Furthermore, the heat transfer from a precessing jet burner is shown to be enhanced relative to a conventional burner and the NO_x emissions reduced if the relationship between heat transfer, emissions and process interaction is taken into account.

To quantify the mixing characteristics of each of the above flows and so to provide insight into the characteristics of relatively "good" and "bad" mixing for the optimisation of combustion in rotary kilns, concentration measurements are performed in a confined, isothermal environment. The effect of co-flow, confinement and the central axial jet on the mixing from a precessing jet nozzle are also assessed. The experiments are performed in a water-tunnel using a quantitative planar laser-induced fluorescence technique to provide measurement of a conserved scalar. The effect of the central axial jet is quantified with respect to its influence upon concentration decay, concentration fluctuations, jet width and probability distribution functions. The effect of co-flow and confinement are also quantified by measurement of the concentration decay, concentration fluctuations, jet width and probability distribution functions. The data is used to develop equations relating the flow conditions and geometry to the mean concentration on the jet axis and jet spread. These equations can be used to describe the entire mean concentration distribution in the far field of the precessing jet flow. Based on the modelling equations, a scaling procedure is proposed that provides a method to scale the precessing jet flow, i.e. to relate isothermal laboratory scale investigations to full scale plant. The scaling procedure is based on a first order assessment of the separate effects of confinement, velocity ratio and mass flow ratio on the scalar mixing. The final scaling parameter represents an additional correction to a modified form of the well known Thring-Newby scaling criterion which distorts the mixture fraction ratio, i.e. the air-fuel ratio, in the model from that in the industrial scale. This correction enables similarity of the jet mixing characteristics to be preserved while correcting for the geometric distortion of the confinement ratio. The new scaling procedure is used to show that the isothermal concentration measurements are representative of the mixing conditions within the pilot-scale combustion facility and hence that the scaling procedure is appropriate for the precessing jet nozzle.

The optimum combustion characteristics of the precessing jet nozzle, defined as the maximum heat transfer and minimum NO_x emissions, are shown to occur at the maximum momentum ratio that still generates a flow characterised as precessing jet dominated. The mixing characteristics associated with high radiation and low NO_x emissions are shown, by the quantitative mixing experiments, to be associated with the maximum mean concentration and the widest range of instantanteous concentrations measured on the jet axis of any flows produced by the combined precessing jet and central axial jet flows. This suggest that such mixing characteristics are desired from any natural gas burner for the maximum heat transfer and minimum emissions in a rotary kiln. The optimal mixing characteristics for the maximum efficieny and lowest emissions from a gas-fired rotary kiln are hence shown to be generated by the precessing jet-central axial jet nozzle at a momentum ratio of $0.17 \leq \Gamma_{CAJ} \leq 0.23$.

Table of Contents

List of Tables

Figure **Page number**

Appendix B

List of Figures

Chapter 4

Chapter 5

Chapter 6

Appendix A

Appendix C

Notation

Abbreviations and Constants

AAJ	Adjacent Annular Jet
ASJ	Annular Shaping Jet
CAJ	Central Axial Jet
CCD	Charge-Coupled Device
$EINO_x$	Emission Index of Nitrogen Oxides
FPJ/PJ	Fluidic Precessing Jet
MCB	Multi-Channel Burner
MPJ	Mechanical Precessing Jet
Nd:YAG	Neodium Yttrium Aluminium Garnet laser
PDF/pdf	Probability Distribution Function
PLIF	Planar Laser-Induced Fluorescence
RMS	Root Mean Square
SNR	Signal to Noise Ratio
σ	Stefan-Boltzmann constant = 5.67×10^{-8}W/m^2.K^4

Roman Symbols

A_{ij}	Correction for the spatial distribution of absorption of laser intensity
b	Absolute path length (m)
$b_{ij}(r)$	Position of pixel (i,j) along the r-axis of a CCD camera image
$b_{ij}(x)$	Position of pixel (i,j) along the x-axis of a CCD camera image
$b_{ij}'(r)$	Corrected position of pixel (i,j) along the r-axis of a CCD camera image
$b_{ij}'(x)$	Corrected position of pixel (i,j) along the x-axis of a CCD camera image
B_{ij}	Spatial distribution of the background noise of a CCD camera
c, C	Fluid concentration
C_{ij}	Fluid concentration measured at pixel location (i,j)
C_{ref}	Reference concentration representing 100% jet fluid
d	Jet exit diameter (m)
d_c	Centre-body diameter (m)
d_{CAJ}	Central axial jet exit diameter (m)
d_ε	Momentum or effective diameter of a jet (m)
d_{or}	PJ nozzle inlet orifice diameter (m)
d_{PJ}	PJ nozzle chamber diameter (m)
d_2	PJ nozzle exit orifice diameter (m)
D	Molecular diffusion coefficient (m^2/s)

D_{duct}	Diameter of a confining duct (m)
D_{kiln}	Diameter of a kiln (m)
f	Frequency (Hz)
f_p	Frequency of precessional motion (Hz)
F	Fluorescence intensity
G	Jet source momentum (N or kg.m/s^2)
G_{CAJ}	Momentum of the central axial jet at the jet exit (N or kg.m/s^2)
G_{ij}	Spatial distribution of the gain response of a CCD camera and optics
G_{PJ}	Momentum of the precessing jet calculated at the upstream orifice inlet to the nozzle chamber (N or kg.m/s^2)
$G_{shaping}$	Momentum of the shaping jet at the jet exit (N or kg.m/s^2)
G_0	The excess momentum flux of a jet relative to the surrounding co-flow (N or kg.m/s^2)
I_{ij}	Spatial distribution of laser intensity
I_0	Incident laser intensity
K_1	Concentration decay constant
K_2	Spreading rate (slope) of the jet concentration half-width
l_{CAJ}	Protrusion distance of the central axial jet exit from the face of the centre-body (m)
l_x	Local length scale in a flow (m)
l_c	Distance between the upstream face of the centre-body and the inlet orifice of the PJ nozzle chamber (m)
l_c	Momentum radius of a jet in a co-flow (m)
L	Chamber length of the PJ nozzle (m)
L	Spatial resolution of a measurement probe or volume (m)
L_{flame}	Flame length (m)
m	Craya-Curtet scaling parameter
$\dot{m}$	Mass flow rate (kg/s)
m_a	Mass flow rate of co-flow/secondary fluid (kg/s)
m_0	Mass flow rate of jet fluid (kg/s)
P_n	Instantaneous laser power in image n
P_{min}	Minimum instantaneous laser power in a set of images
P_{max}	Maximum instantaneous laser power in a set of images
P_{ref}	Calculated reference laser power for the correction of laser power fluctuations
Q	Rate of energy transfer (W)
Q_{rad}	Total measured rate of radiant energy transfer (W)
Q_{loss}	Rate of total heat transfer through the kiln simulator walls (W)
$Q_{wall,abs}$	Rate of radiant energy absorbed by the kiln simulator walls (W)
$Q_{wall,emit}$	Rate of radiant energy transfer emitted by the kiln simulator walls (W)
Q_{flame}	Rate of radiant energy transfer directly emitted by the flame (W)
Q_f	Energy input in the fuel (W)
r	Span-wise (radial) location in cylindrical co-ordinates (m)

r_{CCD}	Size of the CCD array in pixels along the r-axis
r_{break}	Radial distance from the PJ nozzle axis at which the jet edge "breaks" due to the effects of confinement (m)
$r_{1/2}$	Jet centreline concentration half-width (m)
s_c	Ocular distance of the optical system of a CCD camera
S_p	Average signal strength from the laser power reference cell
S_{cref}	Average signal strength from the jet reference concentration cell
$\overline{S}_{ij}$	Spatial distribution of fluorescence intensity
R	Background dye concentration
t	Time (s)
T_f	Non-adiabatic flame temperature (°K)
T_w	Wall surface temperature (°K)
Th	Becker scaling parameter
u	Fluid velocity (m/s)
U	Bulk mean fluid velocity (m/s)
U_a	Bulk mean velocity of co-flow/secondary air or water (m/s)
$U_{e\text{-}PJ}$	Estimated velocity of the precessing jet at the exit of the nozzle chamber (m/s)
U_{or}	Velocity of the precessing jet at the inlet orifice to the PJ nozzle chamber (m/s)
V_{flame}	Flame volume (m^3)
w_c	Axial width of the centre-body (m)
W_{flame}	Maximum flame width (m)
x	Stream-wise (axial) location in cylindrical co-ordinates (m)
x_{break}	Axial distance from the PJ nozzle exit at which the jet edge "breaks" due to the effects of confinement (m)
x_{CCD}	Size of the CCD array in pixels along the x-axis
$x_{0,1}$	Virtual origin based on the inverse concentration (m)
$x_{0,2}$	Virtual origin based on the jet concentration half-width (m)

Greek Symbols

α	Constant of proportionality in the equation relating the Kolmogorov and Batchelor length scales
β	Ratio of the laser power signal strength to the jet reference concentration signal strength
χ	Non-dimensional axial distance on the jet axis, $= (z - z_{0,1})/d_{\varepsilon}$
χ_r	Flame radiant fraction
Δ	Difference
ε	Extinction coefficient of a fluorescent dye
ε	Emissivity
η	Non-dimensional radial distance from the jet axis, $= r/(z - z_{0,2})$
ϕ	Quantum efficiency of a fluorescent dye
Γ^*	Momentum ratio based similarity parameter for swirl and bluff-body nozzles

$\Gamma_{shaping}$	Ratio of shaping jet momentum to the sum of the momentum of the precessing jet, calculated at the upstream orifice inlet to the nozzle chamber, and shaping jet = $G_{shaping}/(G_{PJ} + G_{shaping})$
Γ_{CAJ}	Ratio of central axial jet momentum to the sum of the momentum of the precessing jet, calculated at the upstream orifice inlet to the nozzle chamber, and central axial jet = $G_{CAJ}/(G_{PJ} + G_{CAJ})$
κ	Reference concentration ratio scaling parameter
λ	Resolution length scale (m)
λ_b	Batchelor length scale (m)
λ_k	Kolmogorov length scale (m)
μ	Experimental uncertainty
θ	Thring-Newby parameter
ρ	Fluid density (kg/m^3)
σ	Standard deviation
τ_G	Global flame time scale (s)
τ_b	Batchelor time scale (s)
τ_{pulse}	Laser pulse-fluorescence time scale (s)
τ_{frame}	Laser pulse repetition rate and camera frame rate (s)
ξ	Conserved scalar jet concentration
ξ_{ij}	Conserved scalar jet concentration measured at pixel location (i,j)
$\bar{\xi}$	Mean jet concentration
ξ_{rms}	Root mean square of jet concentration fluctuations
$\psi_{shaping}$	Mass proportion of the total jet flow rate through the shaping jet = $\dot{m}_{shaping}/(\dot{m}_{PJ} + \dot{m}_{shaping})$
ψ_{CAJ}	Mass proportion of the total jet flow rate through the central axial jet = $\dot{m}_{CAJ}/(\dot{m}_{PJ} + \dot{m}_{CAJ})$

Non-Dimensional Parameters

Re	Reynolds number = $\frac{ud}{\nu}$
Sc	Schmidt number = $\frac{\nu}{D}$
Fr	Froude number = $\frac{U}{\sqrt{gl}}$
St_{ex}	Strouhal number of jet excitation = $\frac{fd}{u}$
St_M	Strouhal number of precession from the fluidic precessing jet nozzle, based on jet source momentum = $\frac{f_p\sqrt{\rho}d_{PJ}^2}{\sqrt{G}}$
St_p	Strouhal number of precession from the mechanical precessing jet = $\frac{fd}{U}$

Subscripts

a	Denotes quantity in the co-flow/secondary flow
$e\text{-}PJ$	Estimated quantity for the precessing jet
f	Flame
ij	Denotes quantity at a given pixel (i,j) of a CCD array

min	Minimum value
max	Maximum value
n	n^{th} measurement, e.g. image number
r	radiation
ref	Reference value
rms	Root Mean Square of fluctuating component
w	Wall
0	Denotes quantity at the jet source
∞	Denotes quantity in the ambient environment/far-field
$\bar{}$	Time mean value

Statement of Originality

The material in this thesis is original and has not been submitted or accepted for the award of a degree or diploma at any other university and to the best of my knowledge and belief, the thesis contains no material previously published or written by another person except where due reference is made in the text of the thesis.

Jordan Parham

Permission to Copy

The author consents to the thesis being made available for loan and photocopying provided that the thesis is accepted for the award of the degree.

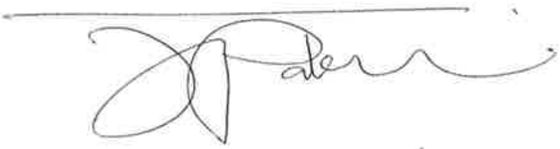

Jordan Parham

Acknowledgment

The completion of this research project has only been possible thanks to the generosity of a wide range of people. In particular, the academic leadership of Emeritus Professor Sam Luxton and Dr. Gus Nathan has successfully guided the research to fruition and contributed significantly to a rewarding research and life experience. The patience, dedication, friendship and inspiration of Gus will always be remembered.

The experiments conducted in this research have benefited significantly from the contributions made by members of the Turbulence, Energy and Combustion (TEC) group. Thanks must go to the many postgraduate students in the TEC group, especially those who have spent time in room S217, for their ideas, assistance and conversation. Dr. David Nobes, Dr. Greg Newbold, Dr. Neil Smith, Mr. Philip Cutler and Mr. Bad Ghazali have especially helped to focus, strengthen and execute the aims of this research. The generosity of Dr. Richard Kelso in providing access to the water-tunnel, image recording and frame-grabbing equipment is most appreciated. The major quantitative mixing experiments would not have been possible without the assistance of Associate Professor Keith King of the Department of Chemical Engineering in securing the Infinity Nd:YAG laser. The contribution of equipment, advice and comments by Dr. David Nobes towards these experiments (which continued from the other side of the world!) was extremely generous. The laser wizardry of Dr. Zeyad Alwahabi ensured the laser based experiments were conducted safely and to the highest standards.

The efforts of the many and varied staff members of the Department of Mechanical Engineering contributed to the development (and repair) of much of the experimental equipment used throughout this research. In particular the contributions of Mr. Graham Kelly, Mr. Anthony Sherry, Mr. Ron Jager, Mr. Craig Price and Mr. Billy Constantine are greatly appreciated. The co-operation and technical input of the staff of the International Flame Research Foundation, especially Mr. Jochen Haas, in conducting the pilot-scale combustion experiments is much appreciated.

This project was made possible by the financial assistance of Fuel and Combustion Technology Ltd. and the Australian Research Council through the Collaborative Grants Scheme. However, the contribution of Fuel and Combustion Technology Ltd. to this research has extended well beyond their financial support. The provision of industrial data, advice, ideas and years of industrial experience from Mr. Steven Hill, Dr. Barrie Jenkins and Dr. Peter Mullinger has ensured a successful commercial and academic outcome from this research.

I am very grateful for the love and support of my partner, Cassie White, and my family who have both helped to share in the highs and lows of the last few years.

Many thanks to you all,

Jordan Parham

Jordan Parham, December 2000